We are IntechOpen, the world's leading publisher of Open Access books Built by scientists, for scientists

6,900
Open access books available

186,000
International authors and editors

200M
Downloads

154
Countries delivered to

Our authors are among the

TOP 1%
most cited scientists

12.2%
Contributors from top 500 universities

CLARIVATE ANALYTICS
BOOK CITATION INDEX
INDEXED

WEB OF SCIENCE™

Selection of our books indexed in the Book Citation Index
in Web of Science™ Core Collection (BKCI)

Interested in publishing with us?
Contact book.department@intechopen.com

Numbers displayed above are based on latest data collected.
For more information visit www.intechopen.com

4

Improved Photochemistry of TiO₂ Inverse Opals and some Examples

Fabrizio Sordello, Valter Maurino and Claudio Minero
Università degli Studi di Torino, Dipartimento di Chimica Analitica, Torino,
Italy

1. Introduction

TiO$_2$ inverse opals are porous TiO$_2$ structures in which the pore arrangement is well ordered in three dimensions. Frequently the pores are arranged in a fcc or hcp structure and each pore is connected to the twelve nearest neighbours. TiO$_2$ commonly occupies about 25% of the volume of the material, while the pores, which can be filled with gaseous or liquid solutions, account for the remaining 75% of the volume (Fig. 1).

The ordered arrangement of pores of the same size can be seen as a periodic modulation of the refractive index in the space, and therefore TiO$_2$ inverse opals are by definition photonic crystals (John 1987; Yablonovitch 1987). Photonic crystals are very useful in controlling the propagation of light, and they can represent for photonics the same improvement semiconductors represented in electronics. Hence properly designed TiO$_2$ inverse opals find application in solar energy recovery (Nishimura et al. 2003; Mihi et al. 2008; Chutinan et al. 2009) and photocatalysis (J. I. L. Chen et al. 2006; Y. Li et al. 2006; Ren et al. 2006; Srinivasan & White 2007; J. I. L. Chen et al. 2008; Sordello et al. 2011a).
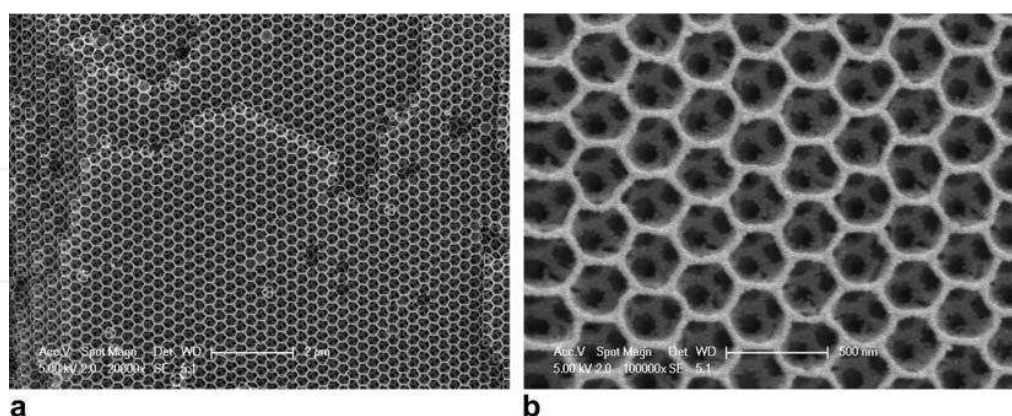

Fig. 1. SEM micrographs of TiO$_2$ inverse opals at different magnification: (a) 20 000x magnification, (b) 100 000x magnification (Reprinted from Waterhouse & Waterland 2007, Copyright (2007), with permission from Elsevier)

This chapter reviews the literature to give a complete picture of the state of the art of the photochemistry on TiO$_2$ inverse opals and outlines the more promising perspectives of the field in the near future.

2. The context: Light driven processes on TiO₂

TiO_2 is used in heterogeneous photocatalysis as photocatalyst in water photosplitting and hydrogen production, in solar cells for the production of electricity, and in other applications that do not require light, such as lithium ion batteries, bone implants and gate insulator for MOSFETs. When TiO_2 is irradiated with light with energy higher than the band gap an electron-hole couple is generated. The charge carriers can separate and migrate towards the surface where they can be trapped or react with solution species, as it can be seen in Fig. 2 (Diebold 2003). Reactive oxygen species are formed, the degradation of organic molecules and pollutants occurs, and the complete mineralization to CO_2, H_2O and inorganic ions has been reported (Pelizzetti et al. 1989). From the environmental point of view this process can be very useful and effective, since the harmful pollutant is not displaced into another phase, but ultimately decomposed to non harmful inorganic compounds. In the presence of a metallic cocatalyst, platinum for example, and in the absence of oxygen, the photogenerated electrons can reduce H_3O^+ to hydrogen, and in the absence of an effective hole scavenger, the photogenerated holes can oxidize water to oxygen, leading to water photosplitting (Ekambaram 2008; Yun et al. 2011). Recently, research focused its attention on the photocatalytic productions of value added chemicals starting from glycerol (Maurino et al. 2008) or directly from CO_2 in artificial photosynthesis (Benniston & Harriman 2008; Roy et al. 2010).

The technological and commercial affirmation of these light driven processes is delayed because (Fujishima et al. 2008; Gaya & Abdullah 2008):

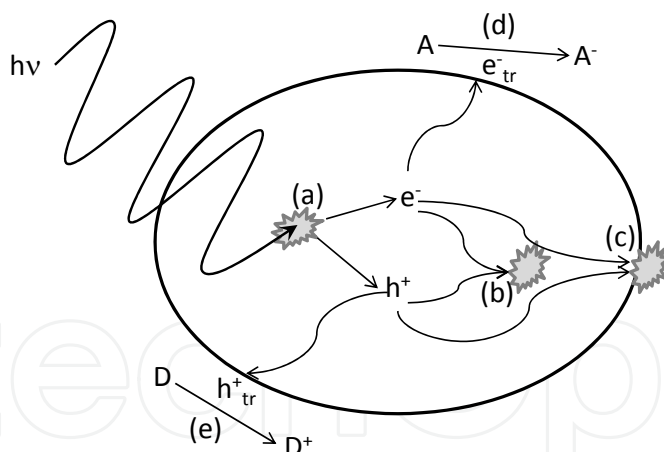1. TiO_2 is an indirect band gap semiconductor, and therefore its light absorption is limited.

Fig. 2. Processes occurring on TiO₂ under UV irradiation: (a) light absorption and charge carriers formation, (b) electron-hole recombination at bulk trapping sites with release of heat, (c) electron-hole recombination at surface trapping sites, (d) trapped electron reacts with acceptor (e) trapped hole reacts with donor.

2. TiO_2 is a wide band gap semiconductor and absorbs only the UV fraction of the solar spectrum.
3. TiO_2 has a quite high refractive index and light absorption is limited also by reflection.
4. The efficiencies of the above mentioned processes are quite low, because the charge carriers recombination is fast.

TiO$_2$ inverse opals can especially improve the light absorption, allowing also a fast mass transfer of solution species due to the large-pore structure. This approach can be combined with other strategies, new or already employed to improve the efficiency of the photocatalytic process on TiO$_2$ surfaces, for example synthesizing doped or dye sensitized TiO$_2$ inverse opals, or realizing structures with controlled exposed surfaces. In this case the achievable structures are limited only by the creativity of the researchers and the synthetic procedures, which can become very complicated and difficult to implement.

In the next section the origin of the better absorption of light of TiO$_2$ inverse opals will be discussed.

3. Photonic band gap and slow photons

As we mentioned in section 1 TiO$_2$ inverse opals are photonic crystals, that is materials characterized by a periodic modulation in the space of the refractive index. The variation of the dielectric constant can be periodic in one dimension, two dimensions or three dimensions. Inverse opals are three dimensional photonic crystals, but for simplicity in the following we will consider the interaction of light with a monodimensional photonic crystal.
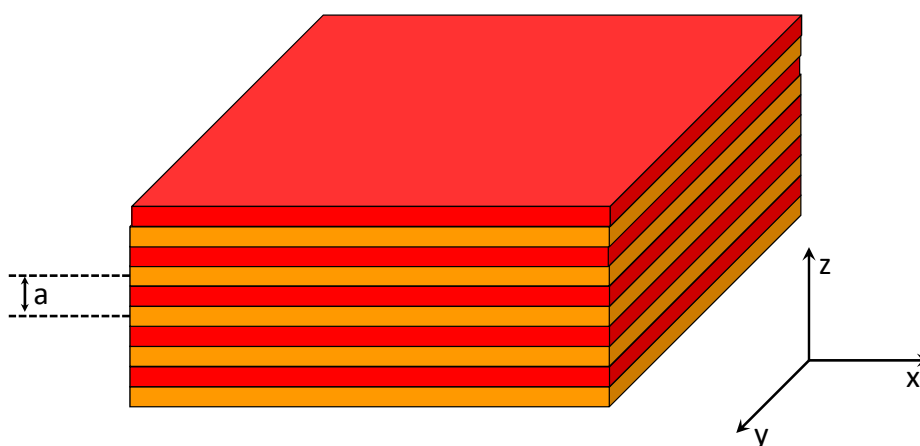

Fig. 3. The multilayer film is a monodimensional photonic crystal. Monodimensional means that the dielectric constant varies only along one direction (z). The system is composed by alternating layers of different materials with different refractive indexes and with spatial period a. Every layer is uniform and extends to infinity along the xy plane. Also the periodicity in the z direction extends to infinity.

A monodimensional photonic crystal is a multilayer film formed by alternating layers of constant thickness, with different refractive index and constant spacing among them (Fig. 3). Referring to Fig. 3 it can be noticed that light propagating in the z direction encounters on its path several interfaces between the two dielectrics. At each interface light is reflected and refracted following the Snell law. If the wavelength of light propagating along the z direction matches perfectly the periodicity of the one-dimensional photonic crystal, the reflected waves will be in phase, and as a consequence i) light will be reflected by the photonic crystal and ii) its propagation inside the material will be forbidden (Yablonovitch 2001). We say that the wavelength (or the frequency) of the incident light falls inside the photonic band gap (Fig. 4).
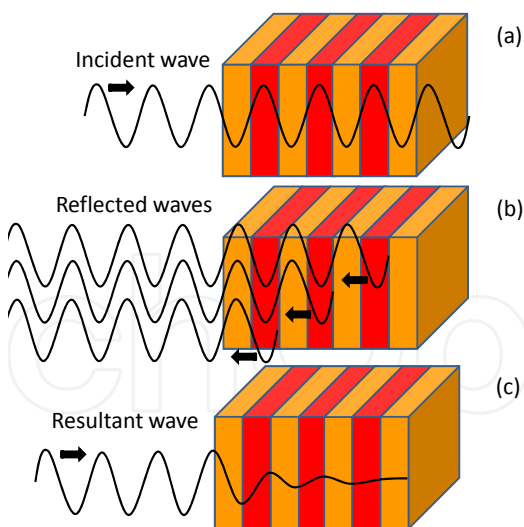
Fig. 4. Schematic representation of an electromagnetic wave impinging a photonic band gap material (a), partial reflection occurs at every interface and, since the frequency of the incident wave falls inside the photonic band gap the reflected waves are all in phase (b); as a result the light cannot travel through the material (c) (adapted from Yablonovitch 2001)
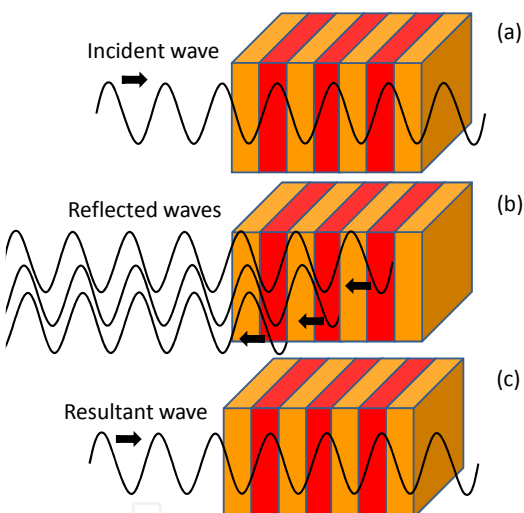

Fig. 5. Schematic representation of an electromagnetic wave with frequency outside the photonic band gap propagating into a photonic crystal (a), in this case the reflected waves are out of phase (b), and the light propagates inside the material only slightly attenuated (c) (adapted from Yablonovitch 2001)

On the contrary, if the wavelength of the incident light does not match the periodicity of the photonic crystal lattice, the waves reflected at each interface will be out of phase, and they will cancel out each other (Fig. 5). As a result the light will be able to propagate inside the material. In this case the wavelength (or the frequency) of the incident light is said to fall outside the photonic band gap.

This approach is useful from a qualitative point of view and gives a general idea of physical phenomena involved, but it cannot be extended to the bidimensional and tridimensional cases. Moreover, it lacks of quantitative understanding of the phenomenon, impeding, for example, the evaluation of the magnitude of the photonic band gap.
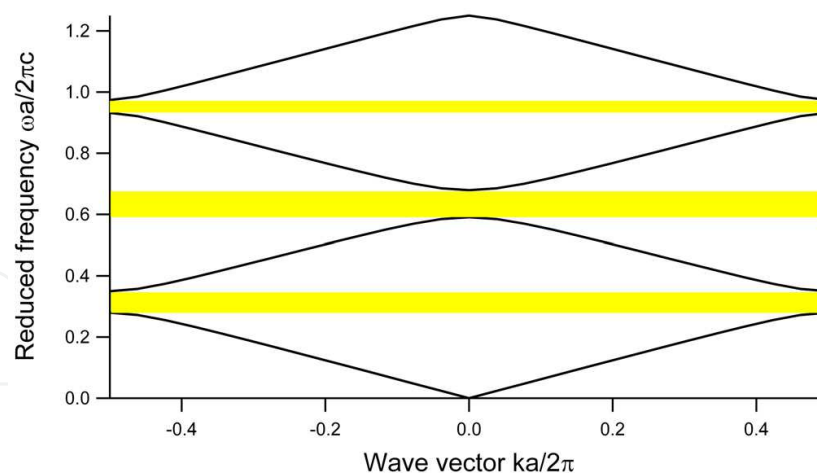
Fig. 6. The photonic band structure of the multilayer film depicted in Fig. 3 calculated with a freely available software (S. G. Johnson & Joannopoulos 2001). The dielectric constants of the layers are ε=5 and ε=2. The photonic band gap frequencies are highlighted in yellow.

A more rigorous approach starts from the treatment of the electromagnetic problem in mixed dielectric media, where the dielectric constant ε(**r**) becomes a function of the spatial coordinate **r**. For this case the Maxwell equations have the form (Joannopoulos et al. 2008):

$$\nabla \cdot \mathbf{H}(\mathbf{r},t) = 0 \tag{1}$$

$$\nabla \cdot [\, \varepsilon(\mathbf{r})\, \mathbf{E}(\mathbf{r},t)] = 0 \tag{2}$$

$$\nabla \times \mathbf{H}(\mathbf{r},t) - \varepsilon_0 \varepsilon(\mathbf{r})\, \partial \mathbf{E}(\mathbf{r},t)/\partial t = 0 \tag{3}$$

$$\nabla \times \mathbf{E}(\mathbf{r},t) + \mu_0\, \partial \mathbf{H}(\mathbf{r},t)/\partial t = 0 \tag{4}$$

where E and H are the macroscopic electric and magnetic fields, $\varepsilon_0 \approx 8.854 \times 10^{-12}$ F/m is the vacuum permittivity, $\mu_0 = 4\pi \times 10^{-7}$ H/m is the vacuum permeability and ε(**r**) is the scalar dielectric function. It can be demonstrated that Maxwell equations can be rearranged to yield equation 5:

$$\nabla \times \{[1/\, \varepsilon(\mathbf{r})]\, \nabla \times \mathbf{H}(\mathbf{r})\} = (\omega/c)^2\, \mathbf{H}(\mathbf{r}) \tag{5}$$

where the electromagnetic problem takes the form of an eigenvalue problem. It can be demonstrated that the operator working on the magnetic field is linear and hermitian. In a mixed periodic medium the eigenfuctions that satisfy equation 5 are in the form of Bloch waves in which the expression of a plane wave is multiplied by a periodic function that accounts for the periodicity of ε(**r**) in the photonic crystal:

$$\mathbf{H}(\mathbf{r}) = e^{i\mathbf{k}\cdot\mathbf{r}}\, \mathbf{u}(\mathbf{r}) \tag{6}$$

where **u**(**r**) is a periodic function of the type **u**(**r**) = **u**(**r**+**R**) for every lattice vector **R** (Joannopoulos et al. 2008). In the case of the multilayer film in Fig. 3 the periodic function u depends only on the z coordinate.

Introducing the Bloch waves of equation 6 in equation 5 the eigenproblem can be solved and the photonic band structure of the photonic crystal of interest can be studied. If in the photonic band diagram there are frequencies for which there are no photonic modes allowed for every wavevector k, a photonic band gap is present (Fig. 6). At those frequencies light cannot propagate inside the material. In such cases the photonic crystals can find application in lasing cavity, optical filter and dielectric mirrors.
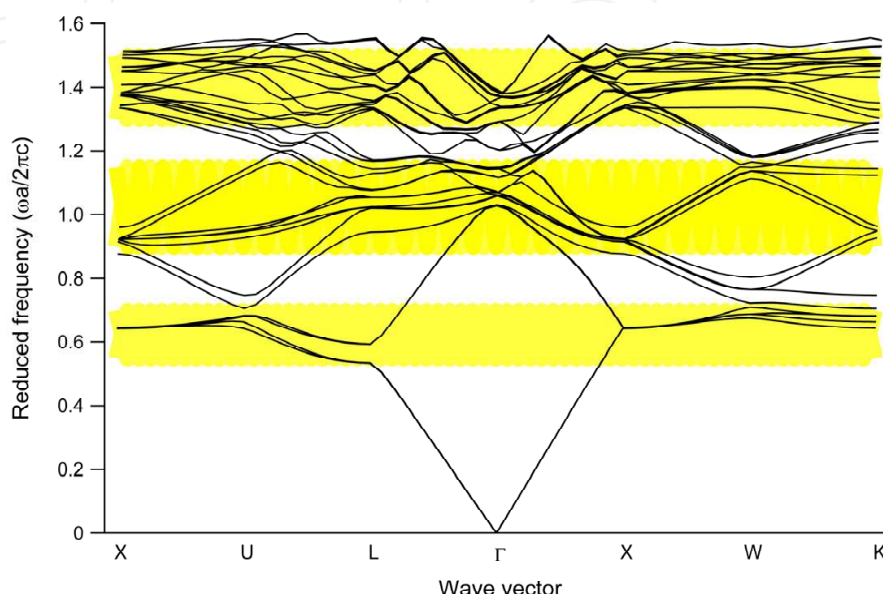

Fig. 7. Photonic band diagram of a TiO$_2$ inverse opal with the pores filled with water. The frequencies associated with light with low group velocity are highlighted. The band structure has been calculated with a freely available software (S. G. Johnson & Joannopoulos 2001) assuming for the dielectric constants of TiO$_2$ and water the values 4.4 and 1.7, respectively.

If equation 5 is solved for the TiO$_2$ inverse opal (Fig. 7) no photonic band gaps are present. To have a photonic band gap in the inverse opal structure the dielectric contrast (the difference between the dielectric constants of the two media) has to be at least 9, whereas TiO$_2$ anatase has a dielectric constant higher than ten only for photon energies above 3.8 – 4.0 eV (310 – 325 nm) (Jellison et al. 2003). Therefore in the visible and UVA TiO$_2$ will not have a complete photonic band gap. Nevertheless, at certain frequencies light will not be able to propagate in some direction (Fig. 7). For example in the Γ-L direction there is a pseudo photonic gap that forbids the propagation of light at a value of the reduced frequency around 0.55. This feature is not so unsuitable for photosynthetic or photocatalytic application, since in those cases light has to propagate inside the catalyst to be absorbed and create charge carriers.

The photonic band diagram of TiO$_2$ inverse opal shows that for some photonic bands the behaviour of the frequency as a function of the wavevector presents an almost flat trend. As the group velocity of light $\mathbf{v_g}$ is defined as:

$$\mathbf{v_g}(\mathbf{k}) = \nabla_{\mathbf{k}}\omega \tag{7}$$

from equation 7 we can argue that a flat trend of a photonic mode in the frequency ω vs. wavevector **k** plot is indicative of low group velocity. Looking at Fig. 7, we can observe that almost flat photonic bands are present for different frequency ranges. At those frequencies light will be able to travel inside the TiO$_2$ inverse opal, but its group velocity will be strongly reduced. Hence the light interaction with the material will be incremented.

When light with low group velocity (or slow light or slow photons) can be exploited, the optical absorption of the material can be improved as if the optical path inside the material would be lengthened. An elegant experimental demonstration of this phenomenon is the change of the absorbance spectrum of an adsorbed dye on different TiO$_2$ inverse opals (Fig. 8).
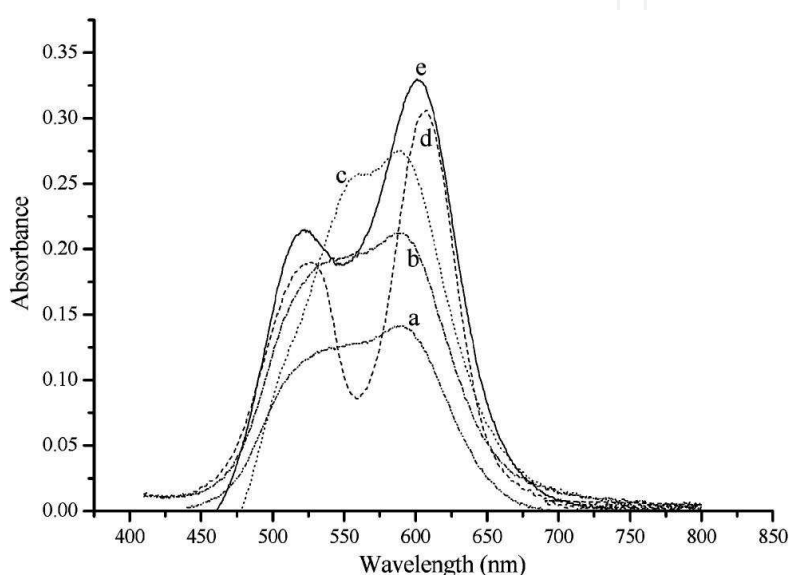

Fig. 8. Absorption spectra of crystal violet adsorbed on different TiO$_2$ films: (a) reference TiO$_2$ flat film, (b) and (c) TiO$_2$ inverse opals slowing photons outside the 450-650 nm range, (d) and (e) TiO$_2$ inverse opals slowing photons in the 600-650 nm range Reprinted with permission from Y. Li et al. 2006 Copyright (2006) American Chemical Society.

When the crystal violet dye is adsorbed on a TiO$_2$ inverse opal, which can slow down the photons possibly absorbed by the dye, its absorbance is increased with respect to flat TiO$_2$ or TiO$_2$ inverse opals with not properly tuned periodicity (Y. Li et al. 2006). Absorption spectra reported in Fig. 8 show that also in the case of TiO$_2$ inverse opals with not properly tuned photonic band gap (slow photons outside the 450-650 nm range) there is a higher absorption that can be explained in terms of porosity and larger amount of adsorbed dye. In the case of TiO$_2$ inverse opals slowing photons in the 600-650 nm range, higher absorption cannot be explained only in terms of porosity and higher amount of adsorbed dye, because not only the intensity of the spectra is different from the reference film, but also because the shape of the spectra changes, as the absorption at 600-625 nm becomes predominant over that at 500 nm.

This important feature, together with porosity and indeed high surface area, makes TiO$_2$ inverse opals very good materials for application in semiconductor photocatalysis, solar energy recovery (dye sensitized solar cells) and artificial photosynthesis (Ren & Valsaraj 2009). Owing to this, they have drawn and they are drawing a lot of research into this field.

4. Synthesis

TiO$_2$ inverse opals can be prepared in several ways and, probably, new synthetic routes will be discovered in the next years. Different approaches are possible because three dimensional ordered porous structures can be obtained exploiting many different physical principles. The invention of new methods is only limited by physics and chemistry and by the creativity of the researchers. An ideal method would be fast, requiring only standard procedures and instruments, it would be cheap and it should be able to produce homogeneous TiO$_2$ inverse opals over large surfaces with the possibility to control the thickness of the synthesized material. A good method would be also able to produce TiO$_2$ inverse opals with few defects both at microscopic (vacancies, dislocations, grain boundaries, stacking faults, ...) and macroscopic level (cracks, thickness inhomogeneity).
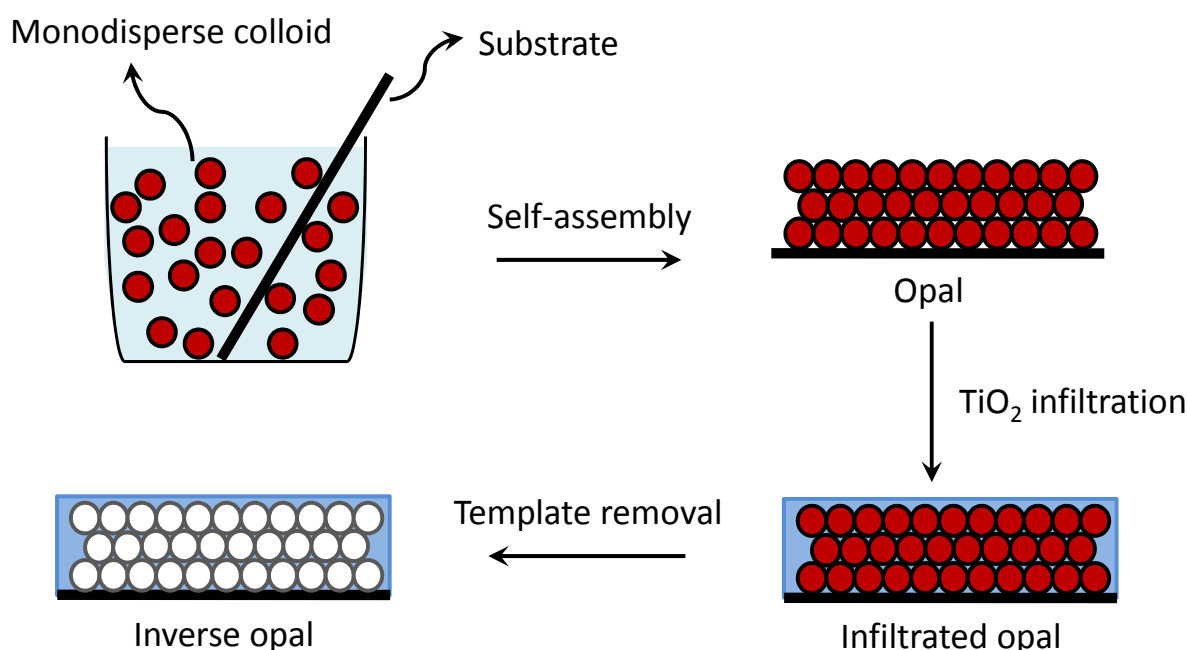

Fig. 9. Schematics of the fabrication procedure of a TiO$_2$ inverse opal.
(adapted from L. Liu et al. 2011)

In general TiO$_2$ inverse opals are synthesized in a two steps procedure (Fig. 9). Firstly, a well monodisperse colloidal suspension of SiO$_2$ or polymer spheres has to be prepared. The monodisperse colloid is then conveniently deposited onto a clean substrate to form a colloidal crystal, that is a solid characterized by an ordered disposition of silica or polymer spheres in three dimensions. A colloidal crystal can be described also as a superlattice of closely packed colloidal particles. If the colloidal particles are spherical the resulting colloidal crystal is called opal or synthetic opal, in analogy with natural opals characterized by an ordered arrangement of silica spheres in three dimensions. Most of the time colloidal crystals obtained in this way are synthetic opals and can find application as sensors (Endo et al. 2007; Shi et al. 2008) and as model systems in the study of crystals, phase transitions (Bosma et al. 2002) and the interaction of photonic crystals with light (Miguez et al. 2004; Pavarini et al. 2005; M. Ishii et al. 2007). Beyond these applications, colloidal crystals serve as sacrificial templates for the synthesis of TiO$_2$ inverse opals. In this case the quality of the colloidal-crystal template is very important, because every defect in the structure will be

replicated in the TiO$_2$ inverse opal. For the TiO$_2$ inverse opal preparation a TiO$_2$ precursor solution (titanium(IV) isopropoxide, titanium(IV) butoxide, other titanium(IV) species) or a dispersion of TiO$_2$ nanoparticles is used to fill the voids of the synthetic opal, a process normally called infiltration. Once the infiltration process is completed and TiO$_2$ backbone is formed, the template is removed by etching with NaOH or HF in the case of silica templates, with toluene in the case of polystyrene templates, or by calcination if a cross linked polymeric template has been used.

4.1 Preparation of monodisperse colloids

In the literature many methods to synthesize monodisperse colloids are described. For the successive colloidal crystal preparation the most suitable method to obtain monodisperse polymeric colloids is the emulsion polymerization without emulsifier in water. To synthesize monodisperse polystyrene colloids the emulsion water-styrene is heated and vigorously stirred, the addition of the initiator makes the reaction start, and the relative amounts of monomer/initiator/ionic strength affect the size of the final polymer spheres (Goodwin et al. 1974). It is also possible to synthesize positively charged polystyrene colloids (Reese et al. 2000) or functionalized colloids (X. Chen et al. 2002) to ease the colloidal crystal formation and the infiltration of TiO$_2$. The preparation of monodisperse polymethylmethacrylate colloids is very similar (Waterhouse & Waterland 2007), and examples of synthesis in non polar solvents are also reported (Klein et al. 2003).

Monodisperse silica spheres can be synthesized in ethanol with determined amount of water in the presence of ammonia as shape controller (Jiang et al. 1999).

4.2 Colloidal crystal synthesis

Many different strategies to obtain colloidal crystals are available depending on the final goal, because they can be obtained as powders, thick films, and also thin films containing one, two or at least three layers.

a. Direct centrifugation of the monodisperse colloid leads to the formation of a colloidal crystal. Although the method is simple, it is not suitable if a film of controlled thickness has to be obtained (Wijnhoven & Vos 1998; Waterhouse & Waterland 2007). Another drawback is the slowness, if small colloidal particles (size < 150 nm) are involved, because more than one hour of centrifugation is needed (Sordello et al. 2011a).

b. A related method is the sedimentation. A drop of the monodisperse colloid is deposited on a clean substrate, where the drop can broaden due to the hydrophilicity of the substrate with contact angle close to zero. The evaporation of the solvent leads to the formation of the colloidal crystal (Denkov et al. 1993). To avoid thickness non uniformity the crystallization can be carried out under silicone liquid (Fudouzi 2004). Since in most cases the evaporation of water is necessary for the synthesis of the colloidal crystal, relative humidity plays an important role (Liau & Huang 2008), and the deposition is quite slow. To accelerate the process ethanol can be used instead of water (Shin et al. 2011).

c. The most popular method used to synthesize colloidal crystals is based on the vertical, rather than horizontal, position of the substrate on which the monodisperse colloid is deposited. When the substrate is dipped into the colloidal dispersion of monodisperse spheres the particles self-assembly in an opaline structure in the meniscus region (Fig.

10). With the evaporation of the solution the meniscus moves downwards and the opal film grows in the same direction (Jiang et al. 1999; Z. Z. Gu et al. 2002; Norris et al. 2004; Shimmin et al. 2006). The method allows the formation of well ordered opals, but the process is slow and the thickness of the film is not uniform, because the colloid concentrates during the process. Moreover, it has been reported that in the vertical deposition method the thickness of the film has a sinusoidal trend in the length scale of the order of 100 μm. The oscillations are more pronounced with increasing particle concentration and with decreasing temperature (Lozano & Miguez 2007).

d. In the dip-drawing technique (Z. Liu et al. 2006) the colloidal crystal is formed by the downwards movement of the meniscus. The substrate is immersed vertical in the colloidal suspension and the meniscus is moved downwards withdrawing the suspension by means of a peristaltic pump. The rapidity of the method can be tuned, but if suspension withdrawal is too fast the quality of the resulting colloidal crystal is poor.

e. Polymer or silica spheres can self assembly in ordered structures in the liquid phase (Reese et al. 2000) forming single crystals over large areas (cm^2) by simply applying a shear flow if the colloidal particles are charged and the ionic strength of the medium is sufficiently low (Amos et al. 2000; Sawada et al. 2001). This method is fast, allows the formation of large single crystals without grain boundaries and, if colloidal particles with opposed charge are employed, colloidal crystals with particle packing different from the usual fcc or hcp geometry are obtained (Leunissen et al. 2005; Shevchenko et al. 2006).
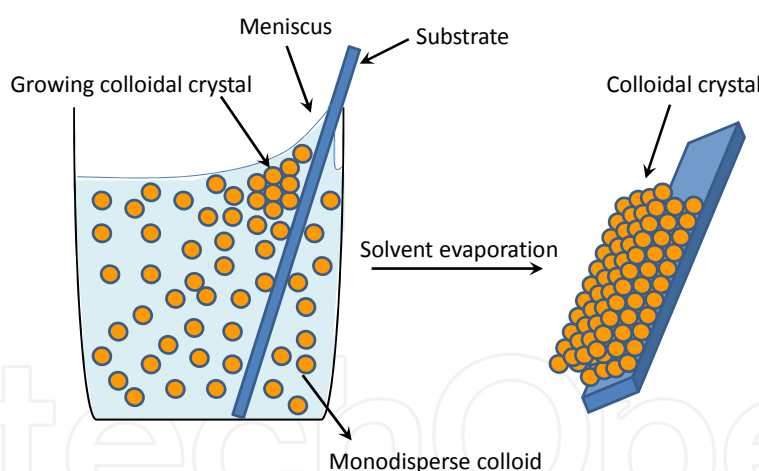

Fig. 10. Schematic representation of a colloidal crystal formed in the meniscus region by slow evaporation of the suspension (adapted from Norris et al. 2004).

The shear flow method can also produce colloidal crystals without cracks over large domains. Normally, once the colloidal crystal is deposited the drying process causes the shrinking of the colloidal particles that produce macroscopic fractures in the structure (Sun et al. 2011). To avoid the formation of these imperfections core-shell spheres can be used. The colloidal crystal is assembled under high external pressure, and during the drying the soft shells will expand, compensating the volume shrinkage of the whole structure (Ruhl et al. 2004; Pursiainen et al. 2008). A further possibility is the use of a photosensitive monomer dissolved in the slurry. The irradiation after colloidal crystal formation will freeze the

structure in a polymeric gel that will prevent any shrinking during the drying process (Kanai & Sawada 2009). These procedures allow the synthesis of almost perfect colloidal crystals over large areas. Nevertheless the subsequent TiO$_2$ infiltration will be considerably hindered.

f. Colloidal crystals are also produced by confinement between two flat surfaces (Fig. 11). The colloidal dispersion of monodisperse spheres can enter the cell because of capillarity forces (M. Ishii et al. 2005; X. Chen et al. 2008) or by means of a hole in the cell (Park et al. 1998; Lu et al. 2001). Evaporation or removal of the solvent with a gas stream leaves behind large area colloidal crystals slightly fractured.
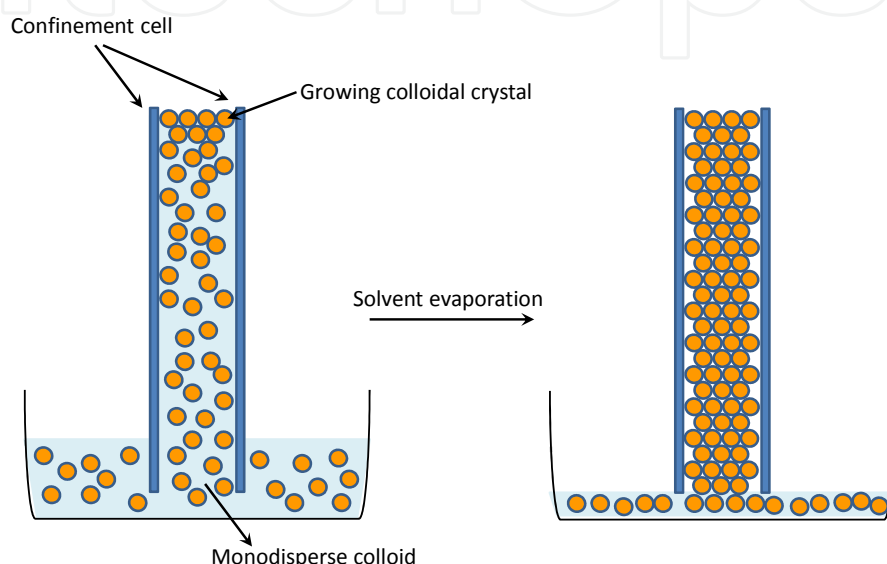

Fig. 11. Schematic representation of the formation of a colloidal crystal in a confinement cell (adapted from X. Chen et al. 2008)

g. Spin coating can be a valuable and rapid method to produce thin film colloidal crystals. Even if many grain boundaries are produced, the distinctive feature of the method is the ability to produce very thin films. The synthesis of monolayered colloidal crystals has been demonstrated (Mihi et al. 2006).

h. Finally, polymeric photonic crystal can also be prepared by mixing immiscible polymers (C. W. Wang & Moffitt 2005) and by laser holographic lithography (Moon et al. 2006; Y. Xu et al. 2008; Lin et al. 2009; Miyake et al. 2009).

4.3 Infiltration and TiO$_2$ inverse opal synthesis

The infiltration in the sacrificial template is the crucial step in the TiO$_2$ inverse opal synthesis, because this phase is responsible for the major production of defects and macroscopic imperfections. If the infiltrated solution or colloid cannot form a stable network before the template is removed, the structure will collapse with the destruction of the three dimensional lattice. Nowadays several infiltration methods exist and in the following we will give the reader a general picture of the available techniques.

The sol-gel infiltration is probably the most popular and widespread method, because it is simple and low cost. Nevertheless, it has to be implemented with great care especially if TiO$_2$

precursors with large tendency to hydrolyze rapidly are used, because the amount of deposited TiO_2 is difficult to control (Wei et al. 2011). In some cases the deposition of an extra layer of bulk TiO_2 over the inverse opal can be turned into an advantage with the lift-off/turn-over method (Fig. 12). Depending on the application both a self standing TiO_2 inverse opal or a Bragg mirror behind a TiO_2 active layer can be created (Galusha et al. 2008). To avoid dealing with violent hydrolysis it is possible to introduce TiO_2 in the template in the form of nanoparticle already hydrolyzed (Yip et al. 2008; Shin et al. 2011). In this case the difficulty is the preparation of sufficiently small particles capable to penetrate into the pores of the opal template, because the resulting infiltration will be poor if the nanoparticles are too big, and the inverse opal structure will collapse after template removal.
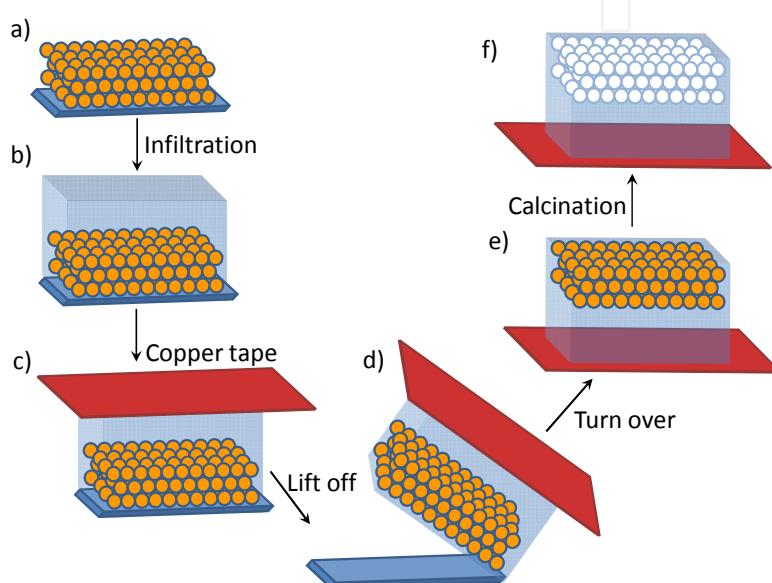

Fig. 12. Schematic representation of the "lift-off/turn-over" technique. (a) polystyrene opal template. (b) Infiltrated opal with TiO_2. (c) Infiltrated opal with adhesive copper tape placed on top. (d) Lift off of the infiltrated opal from the substrate. (e) The infiltrated opal is turned over so that the flat opal-terminated surface is on top. (f) Calcined TiO_2 inverse opal with porous surface (adapted from Galusha et al. 2008).

Electrodeposition is a more complicated method requiring that the sacrificial template is deposited onto a conductive substrate, but it allows a better control of Ti^{4+} hydrolysis and a superior filling of the pores of the template. The potential of the conductive glass that supports the template is brought to negative potential to reduce nitrate present in solution according to the reaction:

$$NO_3^- + 6 \, H_2O + 8 \, e^- \rightarrow NH_3 + 9 \, OH^- \tag{8}$$

The OH^- produced causes a local increase of pH and the precipitation of TiO^{2+} from the precursor solution. In this way the TiO_2 deposition is compact and finely tunable varying the concentration of NO_3^-, the applied current and the deposition time (Y. Xu et al. 2008). A similar technique is electrophoresis. The method can infiltrate a TiO_2 colloid constituted by charged particles, and according to Gu et al. (Z.-Z. Gu et al. 2001), the deposition can be fast and uniform.

Spectacular structures (Fig. 13) can be obtained with infiltration by atomic layer deposition. The technique allows a fine control of the amount of deposited TiO$_2$, the filling of the pores of the template is optimal and, as a consequence, the synthesized TiO$_2$ inverse opals are very resistant. The drawbacks are the slowness and the cost of the needed equipment, which cannot be considered a standard facility of every laboratory (King et al. 2005; L. Liu et al. 2011).

Infiltration can also be carried out by spin-coating, the method is fast and the produced TiO$_2$ inverse opals are regular and characterized by smooth surfaces (Matsushita et al. 2007).
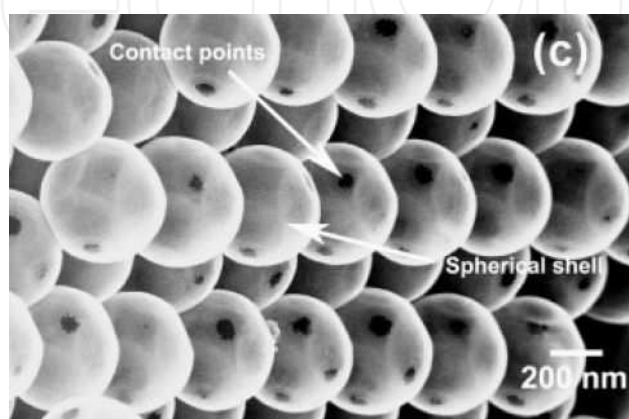

Fig. 13. SEM micrograph of the fractured surface of a TiO$_2$ inverse opal produced by atomic layer deposition (Copyright (2005) Wiley. Used with permission from King at al. 2005)

TiO$_2$ inverse opals can be obtained also in only one synthetic step, in which the silica or polymeric colloid, that will build the colloidal crystal template, is mixed together with a TiO$_2$ colloid that will occupy the interstices of the colloidal crystal structure (Meng et al. 2002). For this reason TiO$_2$ particles have to be one or two orders of magnitude smaller than the silica or polymer particles. The presence of smaller TiO$_2$ particles forces the larger particles to self assembly in close packing. In this way the volume available for the diffusion of the small particles increases, with an overall gain in entropy for the entire system (Yodh et al. 2001).

Beyond the classic filling of TiO$_2$ inverse opal, in which TiO$_2$ occupies the residual volume of the former opal template, a structure also called shell structure or residual volume structure, there are synthetic procedures that can build TiO$_2$ inverse opals with a skeleton structure (Dong et al. 2003) or with a fractal distribution of the pores (Ramiro-Manzano et al. 2007).

5. Improved photochemistry on TiO$_2$ inverse opals

Although the unique properties of TiO$_2$ inverse opals and their possible applications for improved photochemistry are many, surprisingly the first demonstration of better use of light on TiO$_2$ inverse opals dates back only in 2006 (Ren et al. 2006). Before they received attention as back reflector in dye sensitized solar cells (Nishimura et al. 2003; Halaoui et al. 2005; Somani et al. 2005), or in fundamental studies (N. P. Johnson et al. 2001; Schroden et al. 2002; Dong et al. 2003). In that seminal work Ren et al. demonstrated that TiO$_2$ inverse opal

with photonic pseudo gap in the UV is more efficient than P25 TiO_2 in the photodegradation of 1,2-dichlorobenzene in the gas phase (Fig. 14). They also found that the rate constant for the degradation of the pollutant is proportional to the radiant flux intensity even at intensities higher than 25 mW cm⁻², whereas usually for TiO_2 the rate constant is proportional to the square root of the radiant flux intensity (Minero 1999).
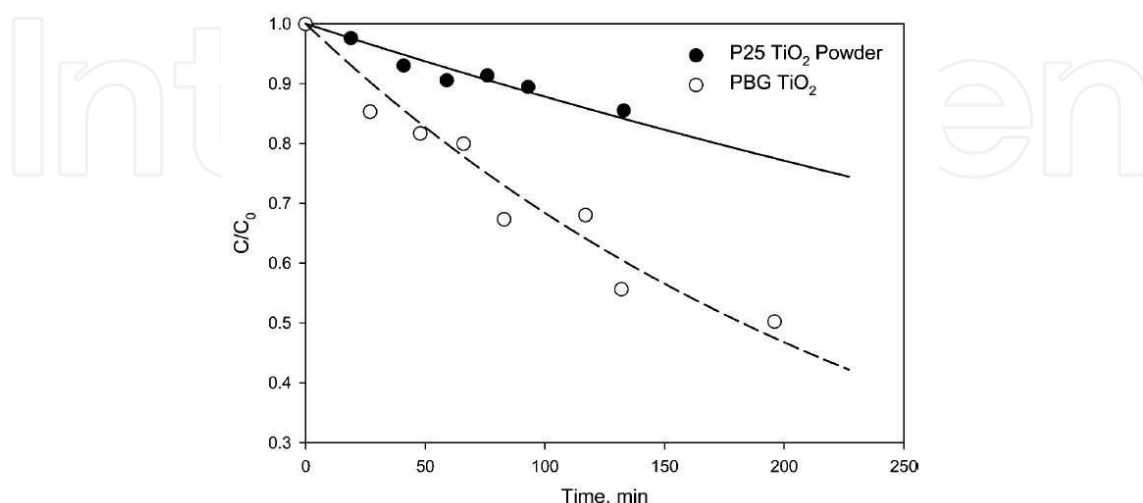

Fig. 14. Normalized concentrations of 1,2-dichlorobenzene as a function of the irradiation time in the presence of P25 TiO_2 powder (closed circles) and TiO_2 inverse opal (PBG TiO_2, open circles) Reprinted with permission from Ren et al. 2006 Copyright (2006) American Chemical Society.
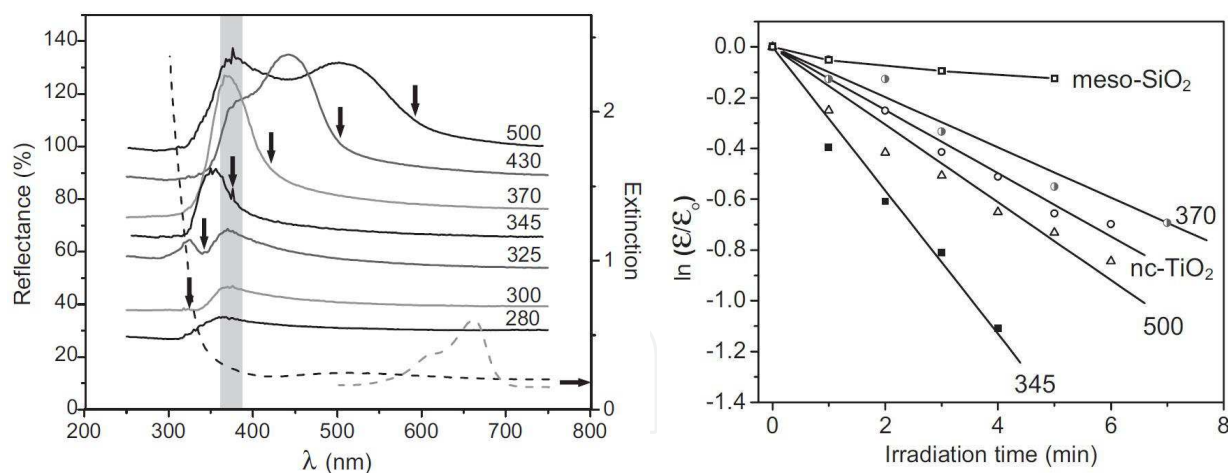

Fig. 15. Left: Reflectance spectra of TiO_2 inverse opals with photonic pseudo gaps located at 500, 430, 370, 345, 325, 300, and 280 nm (solid lines), and extinction spectra of nanocrystalline TiO_2 (black dashed line) and methylene blue (gray dashed line). For clarity the spectra have been displaced in the vertical axis. The highlighted region indicates the wavelengths used during irradiation. Right: Logarithmic plot of the photodegradation of methylene blue showing the first-order decay rate for nanocrystalline TiO_2 (nc-TiO_2) and TiO_2 inverse opals with photonic pseudo gaps at 345, 370, and 500 nm. Mesoporous SiO_2 (meso-SiO_2) was used as the blank (Copyright (2006) Wiley. Used with permission from J.I.L. Chen et al. 2006)

To elucidate the reason of this behaviour Chen et al. (J. I. L. Chen et al. 2006) synthesized TiO$_2$ inverse opals with different pore size, and hence with different position of the photonic pseudo gaps (Fig. 15). The authors observed that with narrow spectrum irradiation (370 ± 10 nm) at the red edge of the photonic pseudo gap the degradation of methylene blue was significantly accelerated with respect to nanocrystalline TiO$_2$, whereas when irradiation was carried out at wavelengths of the photonic pseudo gap the degradation was even slower than in the presence of the reference nanocrystalline TiO$_2$ photocatalyst (Fig. 15). These evidences suggest that the better activity arises from the exploitation of slow photons, which is maximized when the wavelength used for the irradiation falls at the red edge of the photonic pseudo gap, whereas porosity and the improved mass transfer of the species cannot explain such important variations in activity as a consequence of the small difference in the pore sizes used.

The same authors studied also the effect of the disorder on the activity of TiO$_2$ inverse opals (J. I. L. Chen et al. 2007). They found that such systems can tolerate a certain disorder, but the addition in the polymer template of up to 40% of particles with a different diameter (up to 20% different, Fig. 16) leads to a significant loss in activity.
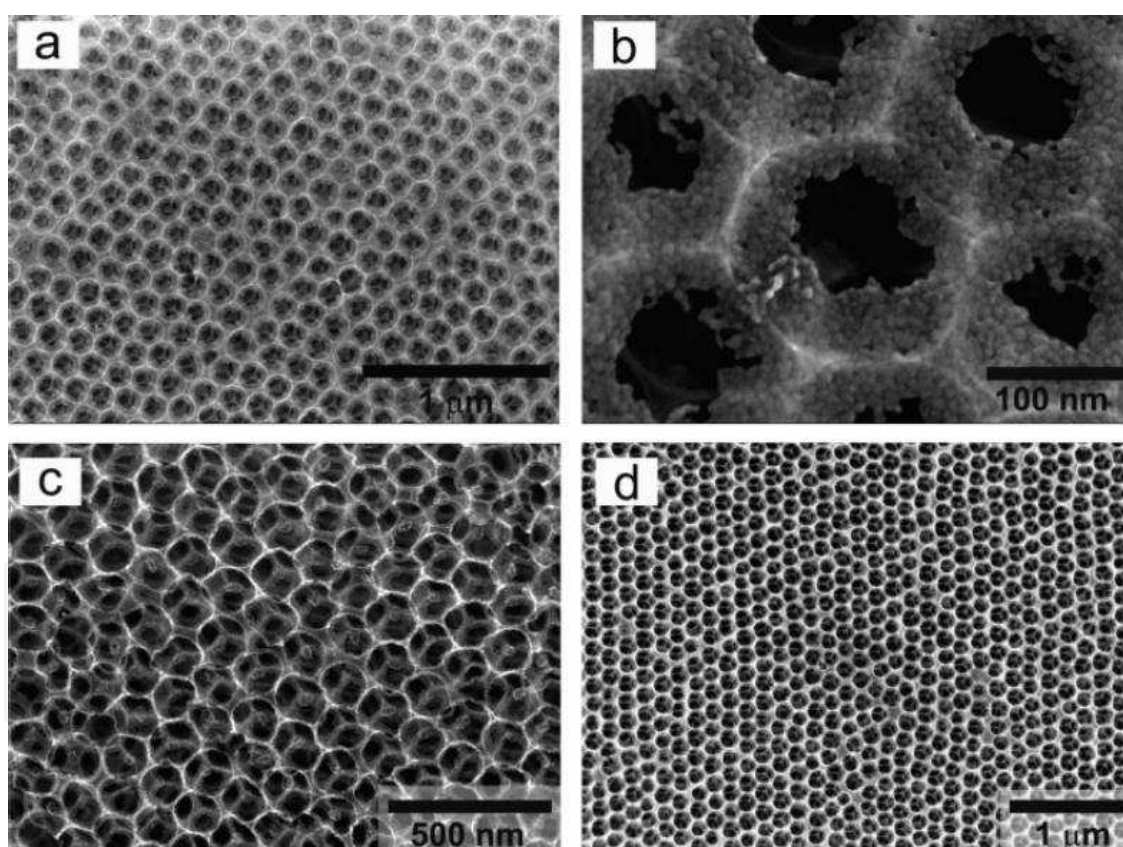
Fig. 16. SEM micrographs of TiO$_2$ inverse opals obtained from PS templates with particle dimensions (1-x)150-x180 nm, with x=0.13 (a and b), 0.37 (c), and 0.57 (d) Reprinted with permission from J.I.L. Chen et al. 2007 Copyright (2007) American Chemical Society.

Nevertheless, partially disordered inverse opals keep an enhancement factor of 1.6, calculated as the activity ratio between TiO$_2$ inverse opal and nanocrystalline TiO$_2$, while the well monodispersed material can attain an enhancement factor of 2.3. This is an

important result because it shows that the light scattering is not crucial in increasing the efficiency of these materials, and that the unavoidable imperfections in the periodic structure do not prevent the practical applications in environmental remediation or water purification.

An improved degradation of methylene blue on TiO_2 inverse opals under UV irradiation was also observed (Srinivasan & White 2007), but in this case the better efficiency was explained in terms of better diffusion of the species due to the porosity of the material and to the large surface area. This interpretation was supported also by Chen & Ozin in a 2009 paper (J. I. L. Chen & Ozin 2009), where they partially revised the conclusions of their previous works, limiting the effectiveness of slow light only in the case of TiO_2 inverse opals with high fill factors.

To clarify the relative importance of slow light, light scattering and improved mass transfer due to the porosity Sordello et al. performed the photocatalytic degradation of phenol at two different wavelengths on TiO_2 inverse opal and TiO_2 disordered macroporous powders (Sordello et al. 2011a). The wavelengths used were 365 nm, where, for the TiO_2 inverse opal employed, the slow photon effect was maximized, and 254 nm, where, on the contrary, the slow light was negligible. At 365 nm the inverse opal is four times more active than the disordered macroporous structure. The key experiment showed that the pristine inverse opal powder is four times more active than the inverse opal crushed in a mortar, which has lost its periodicity in three dimensions. These differences vanish irradiating at 254 nm, as at that wavelength the three powders show almost the same activity. These evidences suggest that slow light plays an important role in increasing the absorption of light of TiO_2 inverse opals and hence in improving their photoactivity. The photoelectrochemical study of TiO_2 inverse opals confirmed the better light absorption of these materials when slow photons are involved. Furthermore, it was evidenced a faster electron transfer to the oxygen present in solution with respect to disordered macroporous TiO_2 (Sordello et al. 2011b).

The better absorption of light, the porosity and the high surface area derive from the structuration of these materials and can be coupled with other physical and chemical modifications to boost efficiency of a great variety of photoreactions. A frequent modification is the addition of metallic platinum to improve the separation of the photogenerated charge carriers and reduce recombination (Kraeutler & Bard 1978). The addition of platinum to TiO_2 inverse opals leads to a significant improvement of the photoactivity (J. I. L. Chen et al. 2008). The activity ratio between platinised inverse opal and nanocrystalline TiO_2 is four, whereas a lower value (around 2.5) should be expected considering the activity ratios of TiO_2 inverse opal (1.7) and platinised nanocrystalline TiO_2 (1.8) alone, evidencing that there is a cooperation between slow light and platinisation. In summary the total effect is not merely the sum of the two contributions (J. I. L. Chen et al. 2008). A different approach consists in synthesizing the metallic platinum inverse opal first, and coating it with TiO_2 in a second step (H. Chen et al. 2010). The recombination of photogenerated charge carriers is effectively reduced by the Schottky junction Pt/TiO_2 as the platinised samples show higher photocurrents and faster photodegradation rate for aqueous phenol. Moreover, Pt/TiO_2 inverse opal with properly tuned photonic pseudo gap has even higher photocurrents and photocatalytic activity with respect to inverse opals that cannot exploit slow light because the irradiation wavelength does not correspond to photonic modes with slow group velocity. It is also interesting to note that without the

chance to harvest slow light Pt/TiO₂ inverse opals have the same characteristics of the macroporous disordered Pt/TiO₂ material (H. Chen et al. 2010).

An alternative strategy used to improve photochemistry on TiO₂ is the doping with transition metals, in order to extend the absorption of light to the visible and to allow practical applications with solar light. Wang et al. (C. Wang et al. 2006) were successful in synthesizing TiO₂, ZrO₂, Ta₂O₅ and Zr or Ta doped TiO₂ inverse opals which were tested in the photocatalytic degradation of 4-nitrophenol and Rhodamine B in aqueous solution. They demonstrated the red shift of the absorption edge of doped TiO₂, and measured higher photoactivity for the doped TiO₂ inverse opal samples. The better activity was attributed to the improved absorption of light due to the doping and to the porosity of the structures constituted by interconnected macropores and mesopores that allow faster migration of photogenerated electrons and holes.
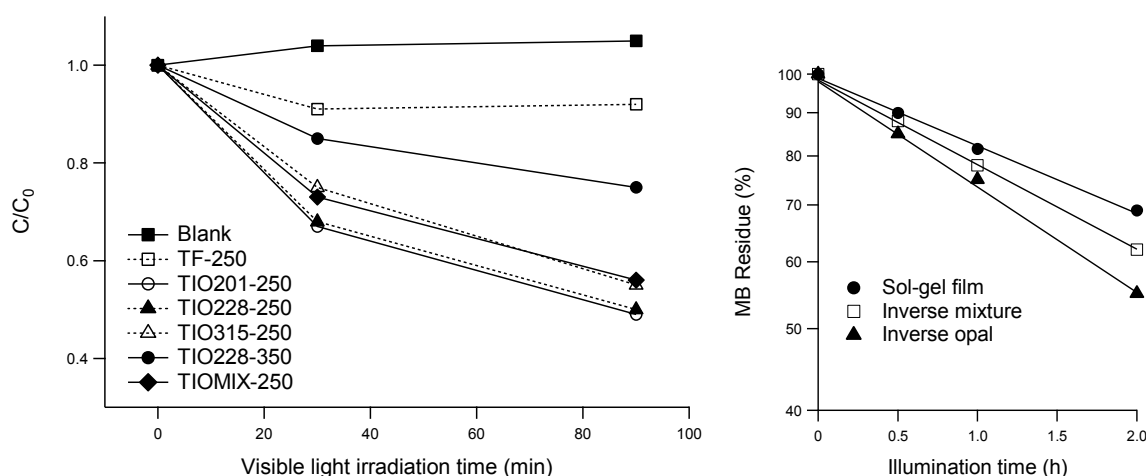

Fig. 17. Left: Methylene blue concentration as a function of the irradiation time for N,F-doped TiO₂ inverse opals with different pore dimensions (e.g. TIO201-250 refers to TiO₂ inverse opal with macropore radius of 201 nm and calcined at 250°C), for a N,F doped TiO₂ macroporous disordered sample (TIOMIX-250), and for N,F doped TiO₂ sol–gel thin film Reprinted with permission from J.A. Xu et al. 2010 Copyright (2010) American Chemical Society. Right: Percent residual methylene blue as a function of the irradiation time (>400 nm) for nitrogen-doped TiO₂ inverse opal (macropore radius ≈ 280 nm), nitrogen-doped TiO₂ macroporous disordered structure (inverse mixture), and nitrogen-doped TiO₂ sol–gel thin film (Copyright (2008) Wiley. Used with permission from Q. Li & Shang 2008)

To extend the absorption of TiO₂ into the visible doping with nitrogen, carbon, sulphur or fluorine is usually adopted. In this case the absorption in the visible is due to colour centres and not to a narrowing of valence and conduction band (Serpone 2006). The doping with nitrogen (Q. Li & Shang 2008) and with nitrogen and fluorine (J. A. Xu et al. 2010) of TiO₂ inverse opal led to an improved photocatalytic degradation of methylene blue in water with visible light, even if in the case of nitrogen and fluorine codoping the activity of the TiO₂ inverse opals is only slightly higher than in the case of a macroporous disordered TiO₂. This is probably due to a non optimal choice of the photonic band gap position, although in the case of nitrogen doping the improvement from disordered to ordered structure is significant (Fig. 17). The photodegradation of methylene blue with visible light alone is not sufficient to demonstrate that doped TiO₂ can effectively absorb visible photons with the consequent

production of holes and electrons that can respectively react with the organic dye and molecular oxygen. According to Zhao et al. (Zhao et al. 2002) the disappearance of the dye is possible under visible light irradiation, without the need of photon absorption by TiO_2. In this case a dye sensitization occurs due to the electron injection from the excited dye (S^*) to the TiO_2 conduction band (equations 9 and 10):

$$S + h\nu \rightarrow S^* \tag{9}$$

$$S^* \rightarrow e^-_{CB} + S^+ \tag{10}$$

The oxidized dye S^+ can directly react with oxygen:

$$S^+ + O_2 \rightarrow SO_2^+ \tag{11}$$

whereas the conduction band electron can react with the dissolved oxygen to yield several reactive oxygen species (Minero & Vione 2006 and references therein):

$$O_2 + e^-_{CB} \rightarrow O_2^{\cdot -} \tag{12}$$

$$O_2^{\cdot -} + H^+ \rightarrow HO_2^{\cdot} \tag{13}$$

$$2\,HO_2^{\cdot} \rightarrow O_2 + H_2O_2 \tag{14}$$

$$O_2^{\cdot -} + HO_2^{\cdot} \rightarrow O_2 + HO_2^- \tag{15}$$

$$H_2O_2 + e^-_{CB} \rightarrow HO^{\cdot} + HO^- \tag{16}$$

$$H_2O_2 + HO^{\cdot} \rightarrow HO_2^{\cdot} + H_2O \tag{17}$$

These species can react with the adsorbed dye and carry out its degradation up to CO_2 and water. In the case of dye molecules adsorbed on the internal surfaces of a TiO_2 inverse opal with properly tuned photonic band gap, dye absorption is enhanced and its degradation improved. This mechanism has been hypothesized to account for the degradation of crystal violet on undoped TiO_2 inverse opal under visible irradiation (Y. Li et al. 2006). The role of the inverse opal is to slow down the photons absorbed by the dye to increase the interaction of light with organic compounds.

TiO_2 inverse opals were also coupled to metallic copper in the photoreduction of CO_2 to methanol in the presence of water vapour and UV light (Ren & Valsaraj 2009). With respect to nanocrystalline TiO_2, on inverse opals the reaction proceeded also at lower light intensities, with a rate dependence on light intensity $I^{0.74}$ with respect to nanocrystalline TiO_2 that showed a dependence $I^{0.20}$.

6. Conclusion

TiO_2 inverse opals and their role in improving the efficiency of photochemical reactions have been presented. The physical origin of the photonic band gap and of slow light has been discussed together with the synthetic routes to obtain such structures. Some applications and practical examples of improved photochemistry on TiO_2 inverse opals have been reviewed, demonstrating how such materials can help photocatalysis to be competitive in solar energy recovery, environmental remediation, water purification and also in the

synthesis of chemicals. The possibility of better light absorption of inverse opals is very promising to improve the efficiency of light driven reactions for a great variety of implementations, provided that knowledge and competences are transferred among different fields. This is a necessary condition to produce complex systems that take advantage of cooperative effects.

7. References

Amos, R. M.; Rarity, J. G.; Tapster, P. R.; Shepherd, T. J. & Kitson, S. C. (2000). Fabrication of large-area face-centered-cubic hard-sphere colloidal crystals by shear alignment. *Physical Review E*, Vol. 61, No. 3, pp. 2929, lSSN:

Benniston, A. C. & Harriman, A. (2008). Artificial photosynthesis. *Materials Today*, Vol. 11, No. 12, pp. 26-34, lSSN: 1369-7021

Bosma, G.; Pathmamanoharan, C.; de Hoog, E. H. A.; Kegel, W. K.; van Blaaderen, A. & Lekkerkerker, H. N. W. (2002). Preparation of Monodisperse, Fluorescent PMMA-Latex Colloids by Dispersion Polymerization. *Journal of Colloid and Interface Science*, Vol. 245, No. 2, pp. 292-300, lSSN:

Chen, H.; Chen, S.; Quan, X. & Zhang, Y. (2010). Structuring a TiO2-Based Photonic Crystal Photocatalyst with Schottky Junction for Efficient Photocatalysis. *Environmental Science & Technology*, Vol. 44, No. 1, pp. 451-455, lSSN: 0013-936X

Chen, J. I. L.; Loso, E.; Ebrahim, N. & Ozin, G. A. (2008). Synergy of slow photon and chemically amplified photochemistry in platinum nanocluster-loaded inverse titania opals. *Journal of the American Chemical Society*, Vol. 130, No. 16, (Apr), pp. 5420-5421, lSSN: 0002-7863

Chen, J. I. L. & Ozin, G. A. (2009). Heterogeneous photocatalysis with inverse titania opals: probing structural and photonic effects. *Journal of Materials Chemistry*, Vol. 19, No. 18, pp. 2675-2678, lSSN: 0959-9428

Chen, J. I. L.; von Freymann, G.; Kitaev, V. & Ozin, G. A. (2007). Effect of Disorder on the Optically Amplified Photocatalytic Efficiency of Titania Inverse Opals. *Journal of the American Chemical Society*, Vol. 129, No. 5, pp. 1196-1202, lSSN:

Chen, J. I. L.; vonFreymann, G.; Choi, S. Y.; Kitaev, V. & Ozin, G. A. (2006). Amplified Photochemistry with Slow Photons. *Advanced Materials*, Vol. 18, No. 14, pp. 1915-1919, lSSN: 1521-4095

Chen, X.; Cui, Z.; Chen, Z.; Zhang, K.; Lu, G.; Zhang, G. & Yang, B. (2002). The synthesis and characterizations of monodisperse cross-linked polymer microspheres with carboxyl on the surface. *Polymer*, Vol. 43, No. 15, pp. 4147-4152, lSSN: 0032-3861

Chen, X.; Sun, Z.; Chen, Z.; Shang, W.; Zhang, K. & Yang, B. (2008). Alternative preparation and morphologies of self-assembled colloidal crystals via combining capillarity and vertical deposition between two desired substrates. *Colloids and Surfaces A: Physicochemical and Engineering Aspects*, Vol. 315, No. 1-3, pp. 89-97, lSSN: 0927-7757

Chutinan, A.; Kherani, N. P. & Zukotynski, S. (2009). High-efficiency photonic crystal solar cell architecture. *Optics Express*, Vol. 17, No. 11, (May), pp. 8871-8878, lSSN: 1094-4087

Denkov, N. D.; Velev, O. D.; Kralchevsky, P. A.; Ivanov, I. B.; Yoshimura, H. & Nagayama, K. (1993). Two-dimensional crystallization. *Nature*, Vol. 361, No. 6407, (07 January 1993), pp. 26, lSSN:

Diebold, U. (2003). The surface science of titanium dioxide. *Surface Science Reports*, Vol. 48, No. 5-8, pp. 53-229, lSSN: 0167-5729

Dong, W. T.; Bongard, H. J. & Marlow, F. (2003). New type of inverse opals: Titania with skeleton structure. *Chemistry of Materials*, Vol. 15, No. 2, (Jan), pp. 568-574, lSSN: 0897-4756

Ekambaram, S. (2008). Photoproduction of clean H2 or O2 from water using oxide semiconductors in presence of sacrificial reagent. *Journal of Alloys and Compounds*, Vol. 448, No. 1-2, pp. 238-245, lSSN: 0925-8388

Endo, T.; Yanagida, Y. & Hatsuzawa, T. (2007). Colorimetric detection of volatile organic compounds using a colloidal crystal-based chemical sensor for environmental applications. *Sensors and Actuators B-Chemical*, Vol. 125, No. 2, (Aug), pp. 589-595, lSSN: 0925-4005

Fudouzi, H. (2004). Fabricating high-quality opal films with uniform structure over a large area. *Journal of Colloid and Interface Science*, Vol. 275, No. 1, pp. 277-283, lSSN: 0021-9797

Fujishima, A.; Zhang, X. & Tryk, D. A. (2008). TiO2 photocatalysis and related surface phenomena. *Surface Science Reports*, Vol. 63, No. 12, pp. 515-582, lSSN:

Galusha, J. W.; Tsung, C. K.; Stucky, G. D. & Bartl, M. H. (2008). Optimizing sol-gel infiltration and processing methods for the fabrication of high-quality planar Titania inverse opals. *Chemistry of Materials*, Vol. 20, No. 15, (Aug), pp. 4925-4930, lSSN: 0897-4756

Gaya, U. I. & Abdullah, A. H. (2008). Heterogeneous photocatalytic degradation of organic contaminants over titanium dioxide: A review of fundamentals, progress and problems. *Journal of Photochemistry and Photobiology C: Photochemistry Reviews*, Vol. 9, No. 1, pp. 1-12, lSSN: 1389-5567

Goodwin, J. W.; Hearn, J.; Ho, C. C. & Ottewill, R. H. (1974). Studies on the preparation and characterisation of monodisperse polystyrene laticee. *Colloid and Polymer Science*, Vol. 252, No. 6, pp. 464-471, lSSN: 0303-402X

Gu, Z.-Z.; Hayami, S.; Kubo, S.; Meng, Q.-B.; Einaga, Y.; Tryk, D. A.; Fujishima, A. & Sato, O. (2001). Fabrication of Structured Porous Film by Electrophoresis. *Journal of the American Chemical Society*, Vol. 123, No. 1, pp. 175-176, lSSN: 0002-7863

Gu, Z. Z.; Fujishima, A. & Sato, O. (2002). Fabrication of high-quality opal films with controllable thickness. *Chemistry of Materials*, Vol. 14, No. 2, (Feb), pp. 760-765, lSSN: 0897-4756

Halaoui, L. I.; Abrams, N. M. & Mallouk, T. E. (2005). Increasing the conversion efficiency of dye-sensitized TiO2 photoelectrochemical cells by coupling to photonic crystals. *Journal of Physical Chemistry B*, Vol. 109, No. 13, (Apr), pp. 6334-6342, lSSN: 1520-6106

Ishii, M.; Harada, M.; Tsukigase, A. & Nakamura, H. (2007). Three-dimensional structure analysis of opaline photonic crystals by angle-resolved reflection spectroscopy. *Journal of Optics a-Pure and Applied Optics*, Vol. 9, No. 9, pp. S372-S376, lSSN: 1464-4258

Ishii, M.; Nakamura, H.; Nakano, H.; Tsukigase, A. & Harada, M. (2005). Large-Domain Colloidal Crystal Films Fabricated Using a Fluidic Cell. *Langmuir*, Vol. 21, No. 12, pp. 5367-5371, lSSN:

Jellison, G. E.; Boatner, L. A.; Budai, J. D.; Jeong, B. S. & Norton, D. P. (2003). Spectroscopic ellipsometry of thin film and bulk anatase (TiO2). *Journal of Applied Physics*, Vol. 93, No. 12, pp. 9537-9541, lSSN: 0021-8979

Jiang, P.; Bertone, J. F.; Hwang, K. S. & Colvin, V. L. (1999). Single-crystal colloidal multilayers of controlled thickness. *Chemistry of Materials*, Vol. 11, No. 8, (Aug), pp. 2132-2140, lSSN: 0897-4756

Joannopoulos, J. D.; Johnson, S. G.; Winn, J. N. & Meade, R. D. (2008). Photonic Crystals Molding the Flow of Light (second), Princeton University Press, 978-0-691-12456-8, Princeton

John, S. (1987). Strong localization of photons in certain disordered dielectric superlattices. *Physical Review Letters*, Vol. 58, No. 23, pp. 2486, lSSN:

Johnson, N. P.; McComb, D. W.; Richel, A.; Treble, B. M. & De la Rue, R. M. (2001). Synthesis and optical properties of opal and inverse opal photonic crystals. *Synthetic Metals*, Vol. 116, No. 1-3, (Jan), pp. 469-473, lSSN: 0379-6779

Johnson, S. G. & Joannopoulos, J. D. (2001). Block-iterative frequency-domain methods for Maxwell's equations in a planewave basis. *Optics Express*, Vol. 8, No. 3, pp. 173-190, lSSN: 1094-4087

Kanai, T. & Sawada, T. (2009). New Route to Produce Dry Colloidal Crystals without Cracks. *Langmuir*, Vol. 25, No. 23, pp. 13315-13317, lSSN:

King, J. S.; Graugnard, E. & Summers, C. J. (2005). TiO2 Inverse Opals Fabricated Using Low-Temperature Atomic Layer Deposition. *Advanced Materials*, Vol. 17, No. 8, pp. 1010-1013, lSSN: 1521-4095

Klein, S. M.; Manoharan, V. N.; Pine, D. J. & Lange, F. F. (2003). Preparation of monodisperse PMMA microspheres in nonpolar solvents by dispersion polymerization with a macromonomeric stabilizer. *Colloid and Polymer Science*, Vol. 282, No. 1, (Dec), pp. 7-13, lSSN: 0303-402X

Kraeutler, B. & Bard, A. J. (1978). Heterogeneous photocatalytic synthesis of methane from acetic acid - new Kolbe reaction pathway. *Journal of the American Chemical Society*, Vol. 100, No. 7, (1978/03/01), pp. 2239-2240, lSSN: 0002-7863

Leunissen, M. E.; Christova, C. G.; Hynninen, A.-P.; Royall, C. P.; Campbell, A. I.; Imhof, A.; Dijkstra, M.; van Roij, R. & van Blaaderen, A. (2005). Ionic colloidal crystals of oppositely charged particles. *Nature*, Vol. 437, No. 7056, pp. 235-240, lSSN:

Li, Q. & Shang, J. K. (2008). Inverse opal structure of nitrogen-doped titanium oxide with enhanced visible-light photocatalytic activity. *Journal of the American Ceramic Society*, Vol. 91, No. 2, (Feb), pp. 660-663, lSSN: 0002-7820

Li, Y.; Kunitake, T. & Fujikawa, S. (2006). Efficient Fabrication and Enhanced Photocatalytic Activities of 3D-Ordered Films of Titania Hollow Spheres. *Journal of Physical Chemistry B*, Vol. 110, No. 26, pp. 13000-13004, lSSN:

Liau, L. C. K. & Huang, Y. K. (2008). Process optimization of sedimentation self-assembly of opal photonic crystals under relative humidity-controlled environments. *Expert Systems with Applications*, Vol. 35, No. 3, (Oct), pp. 887-893, lSSN: 0957-4174

Lin, Y. K.; Harb, A.; Lozano, K.; Xu, D. & Chen, K. P. (2009). Five beam holographic lithography for simultaneous fabrication of three dimensional photonic crystal templates and line defects using phase tunable diffractive optical element. *Optics Express*, Vol. 17, No. 19, pp. 16625-16631, lSSN: 1094-4087

Liu, L.; Karuturi, S. K.; Su, L. T. & Tok, A. I. Y. (2011). TiO2 inverse-opal electrode fabricated by atomic layer deposition for dye-sensitized solar cell applications. *Energy & Environmental Science*, Vol. 4, No. 1, pp. 209-215, lSSN: 1754-5692

Liu, Z.; Ya, J.; Xin, Y.; Ma, J. & Zhou, C. (2006). Assembly of polystyrene colloidal crystal templates by a dip-drawing method. *Journal of Crystal Growth*, Vol. 297, No. 1, pp. 223-227, lSSN:

Lozano, G. & Miguez, H. (2007). Growth Dynamics of Self-Assembled Colloidal Crystal Thin Films. *Langmuir*, Vol. 23, No. 20, pp. 9933-9938, lSSN:

Lu, Y.; Yin, Y.; Gates, B. & Xia, Y. (2001). Growth of Large Crystals of Monodispersed Spherical Colloids in Fluidic Cells Fabricated Using Non-photolithographic Methods. *Langmuir*, Vol. 17, No. 20, pp. 6344-6350, lSSN:

Matsushita, S.; Fujikawa, S.; Onoue, S.; Kunitake, T. & Shimomura, M. (2007). Rapid fabrication of a smooth hollow-spheres array. *Bulletin of the Chemical Society of Japan*, Vol. 80, No. 6, pp. 1226-1228, lSSN: 0009-2673

Maurino, V.; Bedini, A.; Minella, M.; Rubertelli, F.; Pelizzetti, E. & Minero, C. (2008). Glycerol transformation through photocatalysis: A possible route to value added chemicals. *Journal of Advanced Oxidation Technologies*, Vol. 11, No. 2, (Jul), pp. 184-192, lSSN: 1203-8407

Meng, Q. B.; Fu, C. H.; Einaga, Y.; Gu, Z. Z.; Fujishima, A. & Sato, O. (2002). Assembly of Highly Ordered Three-Dimensional Porous Structure with Nanocrystalline TiO2 Semiconductors. *Chemistry of Materials*, Vol. 14, No. 1, pp. 83-88, lSSN: 0897-4756

Miguez, H.; Kitaev, V. & Ozin, G. A. (2004). Band spectroscopy of colloidal photonic crystal films. *Applied Physics Letters*, Vol. 84, No. 8, pp. 1239-1241, lSSN: 0003-6951

Mihi, A.; Calvo, M. E.; Anta, J. A. & Miguez, H. (2008). Spectral response of opal-based dye-sensitized solar cells. *Journal of Physical Chemistry C*, Vol. 112, No. 1, (Jan), pp. 13-17, lSSN: 1932-7447

Mihi, A.; Ocana, M. & Miguez, H. (2006). Oriented colloidal-crystal thin films by spin-coating microspheres dispersed in volatile media. *Advanced Materials*, Vol. 18, No. 17, (Sep), pp. 2244-2249, lSSN: 0935-9648

Minero, C. (1999). Kinetic analysis of photoinduced reactions at the water semiconductor interface. *Catalysis Today*, Vol. 54, No. 2-3, pp. 205-216, lSSN:

Minero, C. & Vione, D. (2006). A quantitative evalution of the photocatalytic performance of TiO2 slurries. *Applied Catalysis B: Environmental*, Vol. 67, No. 3-4, pp. 257-269, lSSN: 0926-3373

Miyake, M.; Chen, Y. C.; Braun, P. V. & Wiltzius, P. (2009). Fabrication of Three-Dimensional Photonic Crystals Using Multibeam Interference Lithography and Electrodeposition. *Advanced Materials*, Vol. 21, No. 29, pp. 3012-+, lSSN: 0935-9648

Moon, J. H.; Yang, S.; Dong, W.; Perry, J. W.; Adibi, A. & Yang, S.-M. (2006). Core-shell diamond-like silicon photonic crystals from 3D polymer templates created by holographic lithography. *Optics Express*, Vol. 14, No. 13, pp. 6297-6302, lSSN:

Nishimura, S.; Abrams, N.; Lewis, B. A.; Halaoui, L. I.; Mallouk, T. E.; Benkstein, K. D.; van de Lagemaat, J. & Frank, A. J. (2003). Standing wave enhancement of red absorbance and photocurrent in dye-sensitized titanium dioxide photoelectrodes coupled to photonic crystals. *Journal of the American Chemical Society*, Vol. 125, No. 20, (May), pp. 6306-6310, lSSN: 0002-7863

Norris, D. J.; Arlinghaus, E. G.; Meng, L.; Heiny, R. & Scriven, L. E. (2004). Opaline Photonic Crystals: How Does Self-Assembly Work? *Advanced Materials*, Vol. 16, No. 16, pp. 1393-1399, lSSN: 1521-4095

Park, S. H.; Qin, D. & Xia, Y. (1998). Crystallization of Mesoscale Particles over Large Areas. *Advanced Materials*, Vol. 10, No. 13, pp. 1028-1032, lSSN: 1521-4095

Pavarini, E.; Andreani, L. C.; Soci, C.; Galli, M.; Marabelli, F. & Comoretto, D. (2005). Band structure and optical properties of opal photonic crystals. *Physical Review B*, Vol. 72, No. 4, pp. 045102, lSSN: 1098-0121

Pelizzetti, E.; Minero, C.; Maurino, V.; Sclafani, A.; Hidaka, H. & Serpone, N. (1989). Photocatalytic degradation of nonylphenol ethoxylated surfactants. *Environmental Science & Technology*, Vol. 23, No. 11, pp. 1380-1385, lSSN:

Pursiainen, O. L. J.; Baumberg, J. J.; Winkler, H.; Viel, B.; Spahn, P. & Ruhl, T. (2008). Shear-Induced Organization in Flexible Polymer Opals. *Advanced Materials*, Vol. 20, No. 8, pp. 1484-1487, lSSN: 1521-4095

Ramiro-Manzano, F.; Atienzar, P.; Rodriguez, I.; Meseguer, F.; Garcia, H. & Corma, A. (2007). Apollony photonic sponge based photoelectrochemical solar cells. *Chemical Communications*, Vol. No. 3, pp. 242-244, lSSN: 1359-7345

Reese, C. E.; Guerrero, C. D.; Weissman, J. M.; Lee, K. & Asher, S. A. (2000). Synthesis of highly charged, monodisperse polystyrene colloidal particles for the fabrication of photonic crystals. *Journal of Colloid and Interface Science*, Vol. 232, No. 1, (Dec), pp. 76-80, lSSN: 0021-9797

Ren, M. M.; Ravikrishna, R. & Valsaraj, K. T. (2006). Photocatalytic degradation of gaseous organic species on photonic band-gap titania. *Environmental Science and Technology*, Vol. 40, No. 22, (Nov), pp. 7029-7033, lSSN: 0013-936X

Ren, M. M. & Valsaraj, K. (2009). Inverse Opal Titania on Optical Fiber for the Photoreduction of CO2 to CH3OH. *International Journal of Chemical Reactor Engineering*, Vol. 7, No. pp. A90, lSSN: 1542-6580

Roy, S. C.; Varghese, O. K.; Paulose, M. & Grimes, C. A. (2010). Toward Solar Fuels: Photocatalytic Conversion of Carbon Dioxide to Hydrocarbons. *ACS Nano*, Vol. 4, No. 3, (Mar), pp. 1259-1278, lSSN: 1936-0851

Ruhl, T.; Spahn, P.; Winkler, H. & Hellmann, G. P. (2004). Large Area Monodomain Order in Colloidal Crystals. *Macromolecular Chemistry and Physics*, Vol. 205, No. 10, pp. 1385-1393, lSSN: 1521-3935

Sawada, T.; Suzuki, Y.; Toyotama, A. & Iyi, N. (2001). Quick Fabrication of Gigantic Single-Crystalline Colloidal Crystals <br> for Photonic Crystal Applications. *Japanese Journal of Applied Physics*, Vol. 40, No. Copyright (C) 2001 The Japan Society of Applied Physics, pp. L1226-L1228, lSSN:

Schroden, R. C.; Al-Daous, M.; Blanford, C. F. & Stein, A. (2002). Optical properties of inverse opal photonic crystals. *Chemistry of Materials*, Vol. 14, No. 8, (Aug), pp. 3305-3315, lSSN: 0897-4756

Serpone, N. (2006). Is the Band Gap of Pristine TiO2 Narrowed by Anion- and Cation-Doping of Titanium Dioxide in Second-Generation Photocatalysts? *The Journal of Physical Chemistry B*, Vol. 110, No. 48, (2006/12/01), pp. 24287-24293, lSSN: 1520-6106

Shevchenko, E. V.; Talapin, D. V.; Kotov, N. A.; O'Brien, S. & Murray, C. B. (2006). Structural diversity in binary nanoparticle superlattices. *Nature*, Vol. 439, No. 7072, pp. 55-59, lSSN:

Shi, J.; Hsiao, V. K. S.; Walker, T. R. & Huang, T. J. (2008). Humidity sensing based on nanoporous polymeric photonic crystals. *Sensors and Actuators B-Chemical*, Vol. 129, No. 1, (Jan), pp. 391-396, lSSN: 0925-4005

Shimmin, R. G.; DiMauro, A. J. & Braun, P. V. (2006). Slow Vertical Deposition of Colloidal Crystals: A Langmuir−Blodgett Process? *Langmuir*, Vol. 22, No. 15, pp. 6507-6513, lSSN: 0743-7463

Shin, J.-H.; Kang, J.-H.; Jin, W.-M.; Park, J. H.; Cho, Y.-S. & Moon, J. H. (2011). Facile Synthesis of TiO2 Inverse Opal Electrodes for Dye-Sensitized Solar Cells. *Langmuir*, Vol. 27, No. 2, pp. 856-860, lSSN: 0743-7463

Somani, P. R.; Dionigi, C.; Murgia, M.; Palles, D.; Nozar, P. & Ruani, G. (2005). Solid-state dye PV cells using inverse opal TiO2 films. *Solar Energy Materials and Solar Cells*, Vol. 87, No. 1-4, (May), pp. 513-519, lSSN: 0927-0248

Sordello, F.; Duca, C.; Maurino, V. & Minero, C. (2011a). Photocatalytic metamaterials: TiO2 inverse opals. *Chemical Communications*, Vol. 47, No. 21, pp. 6147-6149, lSSN: 1359-7345

Sordello, F.; Maurino, V. & Minero, C. (2011b). Photoelectrochemical study of TiO2 inverse opals. *Journal of Materials Chemistry*, Vol. 21, No. 47, pp. 19144 - 19152, lSSN: 0959-9428

Srinivasan, M. & White, T. (2007). Degradation of methylene blue by three-dimensionally ordered macroporous titania. *Environmental Science and Technology*, Vol. 41, No. 12, (Jun), pp. 4405-4409, lSSN: 0013-936X

Sun, W.; Jia, F.; Sun, Z.; Zhang, J.; Li, Y.; Zhang, X. & Yang, B. (2011). Manipulation of Cracks in Three-Dimensional Colloidal Crystal Films via Recognition of Surface Energy Patterns: An Approach to Regulating Crack Patterns and Shaping Microcrystals. *Langmuir*, Vol. 27, No. 13, pp. 8018-8026, lSSN: 0743-7463

Wang, C.; Geng, A.; Guo, Y.; Jiang, S.; Qu, X. & Li, L. (2006). A novel preparation of three-dimensionally ordered macroporous M/Ti (M = Zr or Ta) mixed oxide nanoparticles with enhanced photocatalytic activity. *Journal of Colloid and Interface Science*, Vol. 301, No. 1, pp. 236-247, lSSN: 0021-9797

Wang, C. W. & Moffitt, M. G. (2005). Nonlithographic Hierarchical Patterning of Semiconducting Nanoparticles via Polymer/Polymer Phase Separation. *Chemistry of Materials*, Vol. 17, No. 15, pp. 3871-3878, lSSN: 0897-4756

Waterhouse, G. I. N. & Waterland, M. R. (2007). Opal and inverse opal photonic crystals: Fabrication and characterization. *Polyhedron*, Vol. 26, No. 2, (Jan), pp. 356-368, lSSN: 0277-5387

Wei, N. N.; Han, T.; Deng, G. Z.; Li, J. L. & Du, J. Y. (2011). Synthesis and characterizations of three-dimensional ordered gold- nanoparticle-doped titanium dioxide photonic crystals. *Thin Solid Films*, Vol. 519, No. 8, pp. 2409-2414, lSSN: 0040-6090

Wijnhoven, J. & Vos, W. L. (1998). Preparation of photonic crystals made of air spheres in titania. *Science*, Vol. 281, No. 5378, (Aug), pp. 802-804, lSSN: 0036-8075

Xu, J. A.; Yang, B. F.; Wu, M.; Fu, Z. P.; Lv, Y. & Zhao, Y. X. (2010). Novel N-F-Codoped TiO2 Inverse Opal with a Hierarchical Meso-/Macroporous Structure: Synthesis, Characterization, and Photocatalysis. *Journal of Physical Chemistry C*, Vol. 114, No. 36, pp. 15251-15259, lSSN: 1932-7447

Xu, Y.; Zhu, X.; Dan, Y.; Moon, J. H.; Chen, V. W.; Johnson, A. T.; Perry, J. W. & Yang, S. (2008). Electrodeposition of Three-Dimensional Titania Photonic Crystals from Holographically Patterned Microporous Polymer Templates. *Chemistry of Materials*, Vol. 20, No. 5, pp. 1816-1823, lSSN: 0897-4756

Yablonovitch, E. (1987). Inhibited Spontaneous Emission in Solid-State Physics and Electronics. *Physical Review Letters*, Vol. 58, No. 20, pp. 2059-2062, lSSN:

Yablonovitch, E. (2001). Photonic crystals: Semiconductors of light. *Scientific American*, Vol. 285, No. 6, (Dec), pp. 46-50, lSSN: 0036-8733

Yip, C. H.; Chiang, Y. M. & Wong, C. C. (2008). Dielectric band edge enhancement of energy conversion efficiency in photonic crystal dye-sensitized solar cell. *Journal of Physical Chemistry C*, Vol. 112, No. 23, (Jun), pp. 8735-8740, lSSN: 1932-7447

Yodh, A. G.; Lin, K.-H.; Crocker, J. C.; Dinsmore, A. D.; Verma, R. & Kaplan, P. D. (2001). Entropically Driven Self-Assembly and Interaction in Suspension. *Philosophical Transactions of the Royal Society of London, Series A: Physical Sciences and Engineering*, Vol. 359, No. 1782, pp. 921-937, lSSN:

Yun, H. J.; Lee, H.; Joo, J. B.; Kim, N. D. & Yi, J. (2011). Effect of TiO2 Nanoparticle Shape on Hydrogen Evolution via Water Splitting. *Journal of Nanoscience and Nanotechnology*, Vol. 11, No. 2, (Feb), pp. 1688-1691, lSSN: 1533-4880

Zhao, W.; Chen, C.; Li, X.; Zhao, J.; Hidaka, H. & Serpone, N. (2002). Photodegradation of Sulforhodamine-B Dye in Platinized Titania Dispersions under Visible Light Irradiation: Influence of Platinum as a Functional Co-catalyst. *The Journal of Physical Chemistry B*, Vol. 106, No. 19, (2002/05/01), pp. 5022-5028, lSSN: 1520-6106
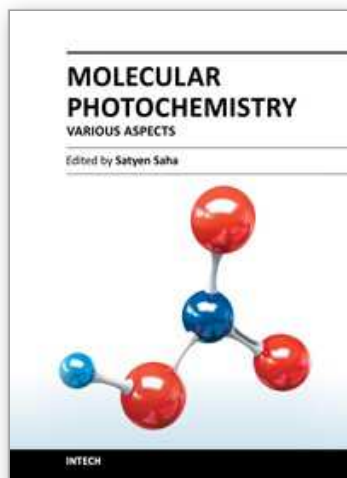
Molecular Photochemistry - Various Aspects

Edited by Dr. Satyen Saha

There have been various comprehensive and stand-alone text books on the introduction to Molecular Photochemistry which provide crystal clear concepts on fundamental issues. This book entitled "Molecular Photochemistry - Various Aspects" presents various advanced topics that inherently utilizes those core concepts/techniques to various advanced fields of photochemistry and are generally not available. The purpose of publication of this book is actually an effort to bring many such important topics clubbed together. The goal of this book is to familiarize both research scholars and post graduate students with recent advancement in various fields related to Photochemistry. The book is broadly divided in five parts: the photochemistry I) in solution, II) of metal oxides, III) in biology, IV) the computational aspects and V) applications. Each part provides unique aspect of photochemistry. These exciting chapters clearly indicate that the future of photochemistry like in any other burgeoning field is more exciting than the past.

How to reference

In order to correctly reference this scholarly work, feel free to copy and paste the following:

Fabrizio Sordello, Valter Maurino and Claudio Minero (2012). Improved Photochemistry of TiO2 Inverse Opals and Some Examples, Molecular Photochemistry - Various Aspects, Dr. Satyen Saha (Ed.), ISBN: 978-953-51-0446-9, InTech, Available from: http://www.intechopen.com/books/molecular-photochemistry-various-aspects/improved-photochemistry-of-tio2-inverse-opals-and-some-examples

INTECH
open science | open minds